



# Optimization of Unidirectional Mucoadhesive Buccal Patches Based on Chitosan and Pluronic® F-127 for Metoprolol Controlled Release: In Vitro and Ex Vivo Evaluations

Cristian Fernando Escalona-Rayo<sup>1</sup> · Pablo Serrano-Castañeda<sup>1</sup> · Miriam López-Cervantes<sup>1</sup> · José Juan Escobar-Chávez<sup>1</sup>

Published online: 30 July 2019

© Springer Science+Business Media, LLC, part of Springer Nature 2019

## Abstract

**Purpose** The aim of this work was to optimize unidirectional buccal patches loaded with metoprolol (MT-MBPs) to provide adequate mucoadhesive and water uptake properties as well as controlled drug release for the effective treatment of different cardiovascular diseases.

**Methods** The patches were prepared layer-by-layer using the solvent casting method. A central composite design was employed to statistically optimize the formulation variables. Chitosan and Pluronic® F-127 (poloxamer 407) concentrations were chosen as the independent variables, while ex vivo mucoadhesive force, ex vivo residence time, in vitro water uptake (%), and in vitro drug release (%) were to be considered the dependent variables. The optimized formulation was also characterized and evaluated in terms of morphology, thermal behavior, tensile strength, elongation at break, and ex vivo drug permeation.

**Results** The optimized MT-MBPs were successful in terms of mucoadhesive force ( $3.58 \pm 0.62$  N), residence time ( $342.67 \pm 17.21$  min), and water uptake at 1 h ( $24.53 \pm 3.62\%$ ). A controlled drug release was obtained for 8 h. Thermal and morphologic analyses demonstrated that metoprolol was homogeneously distributed throughout the microporous chitosan-based polymer matrix. Furthermore, the MT-MBPs exhibited a tensile strength of  $3.76 \pm 0.55$  N/mm<sup>2</sup> and an elongation at break of  $36.52 \pm 13.88\%$ . The results of ex vivo permeation through pig buccal mucosa indicated that therapeutic metoprolol concentrations can be reached by using a patch of 5.62 cm<sup>2</sup>.

**Conclusions** Optimal composition of the MT-MBPs included 2.9% (w/v) and 2.6% (w/v) of chitosan and Pluronic® F-127, respectively, which constitutes the most suitable makeup for metoprolol buccal delivery.

**Keywords** Metoprolol · Cardiovascular diseases · Chitosan · Mucoadhesion · Buccal drug delivery · Unidirectional release

## Introduction

Over the past few decades, the parenteral and per-oral routes have been the most important options for the delivery of several therapeutic agents. However, many drawbacks such as the invasiveness of parenteral delivery and the poor oral bioavailability of some drugs have provoked a search for alternative routes in

order to successfully deliver drugs. In this scenario, buccal drug delivery has emerged as an attractive option for the administration of many drugs, and offers the following advantages: (1) this route of administration is non-invasive and well-accepted by patients, since the buccal cavity is easily reachable for the self-medication and extraction of delivery devices; (2) the buccal mucosa is a well-vascularized tissue with rich blood supply, good permeability, and low enzymatic activity as compared with other mucosal tissues; (3) drugs administered via the buccal route might be rapidly absorbed, avoiding first-pass drug metabolism in the liver and pre-systemic elimination in the gastrointestinal tract, resulting in a higher degree of drug bioavailability with reduced side effects [1–3].

An exemplary buccal drug delivery system should be flexible and possess satisfactory mucoadhesive performance so

✉ José Juan Escobar-Chávez  
josejuanesobar@comunidad.unam.mx

<sup>1</sup> Unidad de Investigación Multidisciplinaria, Laboratorio 12: Sistemas transdérmicos y formas farmacéuticas no convencionales, Carretera Cuautitlán-Teoloyucan, Facultad de Estudios Superiores Cuautitlán Universidad Nacional Autónoma de México, km 2.5 San Sebastián Xhala, C.P. 54714 Cuautitlán Izcalli, Mexico

that it can stay in the buccal cavity for the required period. In addition, drug release from buccal systems should occur in the manner of a controlled and predictable modus to produce the desired therapeutic responses. In recent years, mucoadhesive dosage forms such as tablets, gels, and films have been developed [4–6]. However, mucoadhesive buccal patches (MBPs) may be preferred over mucoadhesive tablets because of their small size, adequate thickness, flexibility, and comfort. Moreover, MBPs are not easily eliminated by saliva like oral gels are [1, 7]. The application of an impermeable backing layer to films ensures a unidirectional drug release and prevents drug loss, minimizing the film disintegration throughout the application period [8].

Even though various polymers have been implemented for the development of mucoadhesive drug delivery systems, chitosan (CS), a biopolymer derived of chitin, has recently received considerable attention owing to its safety and mucoadhesive properties [9]. Poloxamer 407, also known by the trademark name Pluronic® F127 (PF-127), is a nonionic surfactant composed of ethylene oxide (EO) and propylene oxide (PO) blocks organized in a triblock assembly, i.e., EO<sub>100</sub>-PO<sub>65</sub>-EO<sub>100</sub> [10]. PF-127 copolymer exhibits both thermoreversible and bioadhesive properties, which are of the utmost interest in optimizing mucoadhesive drug delivery systems [11].

Metoprolol tartrate (MT) is a water-soluble cardioselective  $\beta$ -blocker recommended in the treatment of different cardiovascular conditions such as hypertension, angina pectoris, cardiac arrhythmias, and myocardial infarction [12]. Although MT is almost comprehensively absorbed after oral administration, its systemic bioavailability (40–50%) can widely fluctuate, owing to extensive first-pass metabolism [13]. MT is comparable with atenolol in terms of lipid solubility ( $\log P$  1.6) and plasma half-life (between 3 and 4 h), making recurrent dosing obligatory in order to preserve the therapeutic blood levels of the drug during long-term treatment [14]. Hence, all these characteristics make this drug a potential candidate for buccal delivery.

The solvent casting method has frequently been used to prepare buccal and transdermal patches, but the formulation variables need to be optimized for increasing the quality of the dosage form. In this context, statistical optimization techniques including response surface methodology (RSM) are widely employed for the development of pharmaceutical formulations in order to estimate the main effects, their interaction, and the quadratic effects of independent variables (factors) on dependent variables (responses) [15–17]. On the other hand, the concept of central composite design (CCD) has been recurrently employed in RSM because it enables the attainment to obtain more information with fewer experiments [18].

According to the literature, no attempt appears to have previously made to formulate unidirectional MBPs

incorporating CS along with PF-127 as a polymer matrix for MT controlled release. Bearing in mind the importance of the buccal drug delivery, the aim of the present investigation was to optimize unidirectional MT-MBPs using such a polymer combination in order to ensure a controlled drug release for a prolonged time as well as to obtain a formulation with satisfactory mucoadhesive and water uptake properties. A CCD was employed to ascertain the effect of formulation variables and to reach an optimized formula. The resultant formulations were characterized for ex vivo mucoadhesive force, ex vivo residence time, in vitro water uptake, in vitro drug release, thickness uniformity, surface pH, folding endurance, moisture content, and drug content. Additionally, the optimized MT-MBPs were characterized and evaluated by way of scanning electron microscopy (SEM), differential scanning calorimetry (DSC), mechanical properties, and ex vivo drug permeation.

## Methods

### Materials

MT was kindly gifted by Bruluart Laboratories (Mexico City, Mexico). CS low molecular weight and 75–85% deacetylated, ethyl cellulose (EC) 48.0–49.5% (w/w) ethoxyl basis, and triacetin were purchased from Sigma-Aldrich (St. Louis, MO, USA). Pluronic® F-127 (PF-127) was purchased from BASF (Mexico City, Mexico). Eudragit® E-100 (Eu-E100) was donated by HELM (Mexico City, Mexico). All other chemicals and solvents were of analytical grade.

### Preparation of the MT-MBPs

The MT-MBPs were prepared layer-by-layer using the solvent casting method [19]. Acetate cellulose molds (12 × 12 cm) were used as molding surfaces. The MT-MBPs included three layers, as follow: a backing layer of EC, an intermediate layer of Eu-E100, and a mucoadhesive layer of CS/PF-127/MT.

**Backing Layer** A backing solution was prepared by gradually adding EC in ethanol 95% under constant magnetic stirring until a 5% (w/v) solution of EC was obtained. This solution was plasticized with triacetin at a concentration of 30% (w/w) based on polymer weight. The formed viscous solution was kept at rest for 30 min to remove any excess air incorporated during stirring. The resultant solution (30 mL) was cast onto an acetate mold and allowed to dry for 3 h at room temperature. The solvent evaporation was regulated by inverting a funnel over the mold.

**Intermediate Layer** A 3% (w/v) solution of Eu-E100 in absolute ethanol was prepared and plasticized with triacetin at a concentration of 20% (w/w) based on polymer weight. The

resultant solution was left at rest for 30 min until a clear, bubble-free solution was obtained. This solution (20 mL) was poured on the backing layer and dried at room temperature. The solvent evaporation was regulated by inverting a funnel over the mold for 2 h.

**Mucoadhesive Layer** CS, PF-127, and MT were dissolved in 2% (v/v) lactic acid. The concentration of plasticizer (glycerol) was kept constant at 5% (w/v). The solution was homogenized and left to stand for 24 h at room temperature enabling the complete hydration of polymers and ensuring a clear, bubble-free solution. This viscous solution (60 mL) was poured on the intermediate layer and allowed to dry for 48 h at room temperature.

The dried patches were detached from the molds and cut into discs (2 cm of diameter), with each disc containing 50 mg of MT. The obtained MT-MBPs were then packed in aluminum foil and stored in a desiccator.

## Experimental Design

To statistically optimize the formulation of MT-MBPs, a three-level, two-factor CCD was employed. The construction and analysis of the experimental design were carried out using the Design Expert® software (version 11.0.3; Stat-Ease Inc., Minneapolis, MN, USA). Based on preliminary trials, the concentrations of CS ( $X_1$ ) and PF-127 ( $X_2$ ) were chosen as independent variables using five distinct levels coded as  $-\alpha$ ,  $-1$ ,  $0$ ,  $+1$ , and  $+\alpha$ . The ex vivo mucoadhesive force ( $Y_1$ ), ex vivo residence time ( $Y_2$ ), in vitro water uptake percentage at 1 h ( $Y_3$ ), and in vitro drug release percentage at 2 h ( $Y_4$ ) were selected as dependent variables. The coded levels, actual levels, and constraints of the variables are shown in Table 1. According to the Design Expert® software, 11 runs were generated and randomly performed to avoid any source of experimental errors. The composition of each formulation as per CCD is displayed in Table 2. The polynomial equation constructed by CCD is given in Eq. 1, as follows:

**Table 1** Independent variables with their levels and dependent variables with their constraints in the CCD

Independent variables	Units	Actual and coded levels				
		$-\alpha$	$-1$	$0$	$1$	$+\alpha$
$X_1 = \text{CS}$	% w/v	0.76	1.30	2.60	3.90	4.43
$X_2 = \text{PF-127}$	% w/v	0.53	0.90	1.80	2.70	3.07
Dependent variables	Units	Constraints				
$Y_1 = \text{Ex vivo mucoadhesive force}$	$N$	$2.0 \leq Y_1 \leq 4.0$				
$Y_2 = \text{Ex vivo residence time}$	min	$360 \leq Y_2 \leq 420$				
$Y_3 = \text{In vitro water uptake after 1 h}$	%	$20 \leq Y_3 \leq 35$				
$Y_4 = \text{In vitro drug release after 2 h}$	%	$40 \leq Y_4 \leq 55$				

**Table 2** Composition of the MT-MBPs as per CCD

Code	Coded levels of factors		Actual levels of factors	
	$X_1$	$X_2$	$X_1$	$X_2$
Factorial points				
1	$-1$	$-1$	1.30	0.90
2	$1$	$-1$	3.90	0.90
3	$-1$	$1$	1.30	2.70
4	$1$	$1$	3.90	2.70
Axial points				
5	$-1.41$	$0$	0.76	1.80
6	$1.41$	$0$	4.43	1.80
7	$0$	$-1.41$	2.60	0.52
8	$0$	$1.41$	2.60	3.07
Center points				
9	$0$	$0$	2.60	1.80
10	$0$	$0$	2.60	1.80
11	$0$	$0$	2.60	1.80

$X_1 = \text{CS} (\% \text{ w/v}); X_2 = \text{PF-127} (\% \text{ w/v})$

$$Y_i = \beta_0 + \beta_1 X_1 + \beta_2 X_2 + \beta_{11} X_1^2 + \beta_{22} X_2^2 + \beta_{12} X_1 X_2 + \varepsilon_i \quad (1)$$

where  $Y_i$  is the predicted response,  $\beta_0$  is the intercept,  $\beta_1$  and  $\beta_2$  are linear coefficients,  $\beta_{11}$  and  $\beta_{22}$  are squared coefficients,  $\beta_{12}$  is the interaction coefficient,  $X_1$  and  $X_2$  are independent variables, and  $\varepsilon_i$  is the term of experimental error.

## Formulation Optimization

Optimal levels of factors were obtained using the Design Expert® software, applying constraints on the mucoadhesive force, residence time, water uptake, and drug release, as shown in Table 1. The objective was to produce patches with adequate mucoadhesive properties and MT controlled release. The optimized formulation was prepared in triplicate to

evaluate the validity of the optimal factors and predicted responses generated by the software. The observed responses were contrasted with the predicted responses and the predicted error percentage was calculated.

### Characterization and Evaluation of MT-MBPs

**Ex Vivo Mucoadhesive Force** For this study, porcine buccal mucosa was selected as a model because of its resemblance to human buccal mucosa [20]. Porcine buccal mucosa was obtained from a local slaughterhouse and transported in simulated salivary fluid (SSF) with a pH of 6.8. After the removal of fatty layers by scalpel, the buccal mucosa was isolated from the underlying tissue, cleaned with SSF, and immediately used for testing. To determine ex vivo mucoadhesive force, a texture analyzer (Brookfield CT3; AMETEK Brookfield, Middleborough, MA, USA) was employed. Patches were firmly attached to the probe with double-sided tape so that the CS/PF-127/MT mucoadhesive layer made contact with the buccal mucosa. The test was carried out by applying an activation charge of 6.8 g for 60 s. The probe was then removed from the mucosa at a speed 2 mm/s while obtaining the force necessary to detach the patch from porcine buccal mucosa. This procedure was performed for six patches from each formulation, and the mean mucoadhesive force was reported.

**Ex Vivo Residence Time** The ex vivo residence time was obtained after application of the MT-MBPs on porcine buccal mucosa previously fixed on a glass beaker using cyanoacrylate glue. The glass beaker was then filled with 200 mL of SSF and maintained at  $37 \pm 0.5$  °C under a stirring rate of 150 rpm. These conditions simulated the buccal cavity environment [21]. The test was halted when patches were detached from the mucosa. Three MT-MBPs of each formulation were evaluated.

**In Vitro Water Uptake Studies** Patches were individually weighed ( $W_1$ ) and dipped in 2 mL of SSF for predetermined time periods. The patches were then removed, the excess surface SSF was wiped off with filter paper, and the patches were reweighed ( $W_2$ ). The water uptake percentage of the MT-MBPs was calculated at each time point according to Eq. 2 [22], as follows:

$$\text{Water uptake (\%)} = \left( \frac{W_2 - W_1}{W_1} \right) \times 100 \quad (2)$$

**In Vitro Drug Release Studies** The in vitro release of MT from the MT-MBPs was carried out using a USP apparatus V (paddle over disc) dissolution system (APPM-0250; Mayasa, Mexico City, Mexico). The release medium was 900 mL of 20 mM phosphate buffer (pH 7.4) maintained

at  $37 \pm 0.5$  °C and 50 rpm of stirring. Patches were placed on the disc in such a way that only the mucoadhesive layer was in contact with the release medium. At programmed time intervals, a volume of 3 mL of release medium was withdrawn and substituted with fresh medium. The samples were filtered and analyzed spectrophotometrically at a  $\lambda_{\text{max}}$  of 219 nm. The drug release percentage was estimated with a standard calibration curve of MT in phosphate buffer (range 8.53–85.36  $\mu\text{g/mL}$ ,  $y = 0.0255x + 0.0040$  and  $R\text{-squared} = 0.9986$ ). The cumulative drug release was plotted versus time. Likewise, in vitro drug release, data were fitted to different kinetic models such as order zero, first order, Higuchi, and Korsmeyer–Peppas. The model with the highest correlation coefficient was contemplated to be the best-fitting one.

**Thickness and Surface pH** The thickness of the MT-MBPs was measured at five distinct areas per patch by using a digital vernier caliper (CALDI-6MP; Truper, Mexico City, Mexico) and a mean thickness of 10 patches was reported. The surface pH of the MT-MBPs was determined to evaluate the compatibility with the physiological pH of the buccal mucosa. The MT-MBPs were dipped in 5 mL of SSF, and after 2 h, the pH was measured by placing the electrode in contact with the mucoadhesive surface [23]. The mean of three measurements for each batch was reported.

**Folding Endurance and Moisture Content** The folding endurance test was manually realized by folding patches repeatedly at a 180° angle until their fracture was observed. The number of folds needed to fracture the patches was expressed as the value of folding endurance [24]. For the determination of moisture content, the MT-MBPs were individually weighed ( $W_1$ ) and kept in a desiccator with anhydrous calcium chloride. After 3 days, the MT-MBPs were reweighed ( $W_2$ ). The moisture content percentage was calculated using Eq. 3 [25], as follow:

$$\text{Moisture content (\%)} = \left( \frac{W_1 - W_2}{W_1} \right) \times 100 \quad (3)$$

The folding endurance and moisture content evaluations were completed in triplicate for each formulation.

**Determination of Drug Content** The MT-MBPs were dissolved in 100 mL of phosphate buffer containing 2 mL of 2% (v/v) lactic acid under constant magnetic stirring. The solutions were filtered and then analyzed spectrophotometrically at  $\lambda_{\text{max}}$  219 nm for verifying the real amount of MT in the MT-MBPs. The results were expressed as the mean percentage of three measurements of each batch.



## Characterization and Evaluation of the Optimized MT-MBPs

The optimized MT-MBPs were characterized regarding the features mentioned above as well as considering the following.

**SEM Study** Surface morphology of the optimized MT-MBPs was examined by SEM using a microscope (JSM-6010LA; JEOL, Peabody, MA, USA). The samples were coated with a golden layer and then seen under the SEM microscope.

**DSC Study** Solid state and thermal behavior of raw materials and optimized formulation were studied by DSC using a differential scanning calorimeter (DSC822e; Mettler Toledo, Columbus, OH, USA). A heating rate of 10 °C/min was employed at a range of –25 °C to 250 °C under an inert atmosphere of nitrogen. The thermograms of MT, CS, PF-127, and optimized MT-MBPs were obtained.

**Measurement of Mechanical Properties** Mechanical properties of the optimized MT-MBPs were analyzed using the texture analyzer. Strips (80 × 20 mm) from patches were positioned between two clamps separated by a distance of 30 mm. Breaking force and elongation at break were designated as when the MT-MBPs broke via the application of a load cell speed of 0.5 mm/s. The tensile strength and elongation at break were calculated by Eqs. 4 and 5, respectively [26]:

$$\begin{aligned} \text{Tensile strength (N/mm}^2\text{)} \\ = \frac{\text{Breaking force (N)}}{\text{cross sectional area of sample (mm}^2\text{)}} \quad (4) \end{aligned}$$

$$\begin{aligned} \text{Elongation at break (\%)} \\ = \frac{\text{Increase in length at braking point (mm)}}{\text{Initial length (mm)}} \times 100 \quad (5) \end{aligned}$$

**Ex Vivo Drug Permeation Studies** The ex vivo permeation studies through buccal porcine mucosa were conducted involving vertical Franz-type diffusion cells with an effective diffusional area of 2.01 cm<sup>2</sup>. The porcine buccal mucosa was placed between both compartments of the cells and the mucoadhesive layer of the MT-MBPs was fixed in the tissue. The receptor compartment was filled with phosphate buffer and maintained at 37 ± 0.5 °C under magnetic stirring of 50 rpm. At programmed periods of time, samples of 1 mL were collected and substituted with fresh medium. The amount of permeated drug was analyzed by spectrophotometry at λ<sub>max</sub> 219 nm. The cumulative amount of drug permeated per unit area (*Q*, mg/cm<sup>2</sup>) as a function of time (h) was plotted. The steady state flux (*J*<sub>SS</sub>, μg/cm<sup>2</sup>/h) of MT was estimated

from the slope of the graph by linear regression analysis. The lag time (*t*<sub>L</sub>) was ascertained from the *x*-intercept of the slope obtained for the estimation of the *J*<sub>SS</sub>. The permeability coefficient (*K*<sub>p</sub>, cm/h) of the drug through mucosa was calculated by dividing *J*<sub>SS</sub> by initial drug concentration in the MT-MBPs [27].

## Results and Discussion

### Preparation and Optimization of MT-MBPs

The MT-MBPs were successfully prepared using the solvent casting method, which is a technology that is well established and widely used today for manufacturing patches. The EC backing layer was incorporated into the CS/PF-127/MT mucoadhesive layer to obtain unidirectional MT release and prevent drug swallowing, while the Eu-E100 intermediate layer functioned as an adhesive between the mucoadhesive and backing layers. The obtained MT-MBPs exhibited a transparent, homogeneous, flexible appearance and were easily detached from the molding surface.

**Statistical Analysis of CCD and Interpretation** CCD-RSM was utilized for optimizing the formulation variables of the MT-MBPs. Table 3 displays the observed responses for all of the formulations prepared as per CCD. Data of responses (*Y*<sub>1</sub>–*Y*<sub>4</sub>) were fitted to linear, 2FI, and quadratic models, where the election of the best-fit model was validated using an analysis of variance test (ANOVA) and by the highest *R*-squared and adjusted *R*-squared values. The *P* values (< 0.05) indicated that the quadratic model was significant for fitting all four responses. Additionally, the *R*-squared and adjusted *R*-squared values for all four responses were in the range of 0.8939 to 0.9688 and 0.7877 to 0.9375, respectively, indicating good correlation and a significant fit in the case of the quadratic model (Table 4). The estimate coefficients with *P* < 0.05 of the generated polynomial equations were considered to be statistically significant. Positive coefficients indicated a direct correlation between factors and responses. On the contrary, negative coefficients implied an inverse correlation between factors and responses.

**Ex Vivo Mucoadhesive Force** The mucoadhesive force is a relevant parameter frequently employed to describe the maximum force needed to detach mucoadhesive delivery systems from buccal mucosa. The ex vivo mucoadhesive force (*Y*<sub>1</sub>) of the MT-MBPs ranged between 0.68 ± 0.19 and 9.82 ± 0.74 N, as shown in Table 3. The full model equation describing the relationship between factors and this response is depicted in Eq. 6, as follows:

**Table 3** Observed responses and characterization of the MT-MBPs prepared as per CCD

Code	$Y_1$ (N) <sup>a</sup>	$Y_2$ (min) <sup>b</sup>	$Y_3$ (%) <sup>b</sup>	$Y_4$ (%) <sup>b</sup>	Thickness (μm) <sup>c</sup>	Surface pH <sup>b</sup>	Folding endurance (No.) <sup>b</sup>	Moisture content (%) <sup>b</sup>	Drug content (%) <sup>b</sup>
F1	1.44 ± 0.28	230.67 ± 20.55	64.27 ± 10.26	84.48 ± 4.35	760 ± 53.12	6.22 ± 0.18	236 ± 11	3.30 ± 0.68	96.74 ± 0.81
F2	9.23 ± 0.44	437.67 ± 23.44	36.31 ± 63.89	67.64 ± 4.83	789 ± 47.95	6.24 ± 0.15	266 ± 18	2.89 ± 0.32	97.27 ± 1.03
F3	1.14 ± 0.21	324.67 ± 28.36	28.45 ± 2.21	62.17 ± 6.22	587 ± 35.92	6.33 ± 0.12	270 ± 12	3.53 ± 0.59	97.29 ± 0.72
F4	9.70 ± 0.60	387.33 ± 32.25	21.32 ± 4.74	46.47 ± 6.25	776 ± 59.10	6.13 ± 0.18	246 ± 12	3.28 ± 0.90	97.73 ± 1.29
F5	0.68 ± 0.19	114.67 ± 20.03	61.43 ± 8.08	74.63 ± 3.77	646 ± 32.39	6.02 ± 0.18	251 ± 12	2.37 ± 0.23	95.27 ± 1.77
F6	9.82 ± 0.74	442.67 ± 36.67	26.41 ± 2.46	48.89 ± 3.89	756 ± 69.79	6.10 ± 0.16	253 ± 10	2.10 ± 0.34	97.05 ± 1.65
F7	2.53 ± 0.32	388.67 ± 23.54	59.93 ± 5.38	70.01 ± 5.36	781 ± 49.54	6.01 ± 0.11	264 ± 19	2.59 ± 0.51	97.74 ± 1.75
F8	3.54 ± 0.35	315.33 ± 29.86	19.31 ± 5.55	44.43 ± 3.96	762 ± 46.14	6.16 ± 0.14	272 ± 14	2.54 ± 0.45	96.95 ± 0.78
F9	2.52 ± 0.23	340.33 ± 38.10	35.34 ± 3.78	65.61 ± 4.25	722 ± 43.78	6.10 ± 0.17	241 ± 18	2.98 ± 0.55	95.72 ± 1.71
F10	2.56 ± 0.39	351.33 ± 23.61	38.32 ± 4.26	69.31 ± 4.72	781 ± 39.85	6.21 ± 0.11	257 ± 15	3.50 ± 0.34	97.41 ± 1.48
F11	2.54 ± 0.36	360.67 ± 28.98	32.86 ± 3.71	66.76 ± 5.02	769 ± 41.75	6.29 ± 0.12	265 ± 14	3.80 ± 0.75	96.52 ± 1.37

$Y_1$  = Ex vivo mucoadhesive force;  $Y_2$  = Ex vivo residence time;  $Y_3$  = In vitro water uptake after 1 h;  $Y_4$  = In vitro drug release after 2 h

<sup>a</sup> Values are presented as mean ± SD,  $n = 6$

<sup>b</sup> Mean ± SD,  $n = 3$

$$Y_1 = 2.54 + 3.66X_1 + 0.19X_2 + 0.19X_1X_2 + 1.66X_1^2 + 0.55X_2^2 \quad (6)$$

The factor  $X_1$  had significant positive linear and quadratic effects on the response  $Y_1$  (Table 4), indicating that the patches with the highest content of CS markedly increased the mucoadhesive force. This observation could be attributed to the fact that CS possesses a large number of –OH and –NH<sub>2</sub> groups that confer mucoadhesive properties. These properties can be explained first by the diffusion–interpenetration of CS

chains on the mucosal surface, followed by the formation of both hydrogen bonds and electrostatic interactions between –OH and –NH<sub>2</sub> groups and mucus components [28]. Hydrophobic interactions might also contribute to the mucoadhesive properties of CS [29]. In addition, by increasing the CS concentration, the available sites for the formation of secondary interactions also increased, which led to a high mucoadhesive force. Three-dimensional (3D) response surface and contour plots showing the effects of the factors on the ex vivo mucoadhesive force are presented in Fig. 1a and b.

**Table 4** Fit to linear, 2FI, and quadratic models for  $Y_1$  to  $Y_4$  along with the estimated effect of factors and associated  $P$  values for the quadratic model

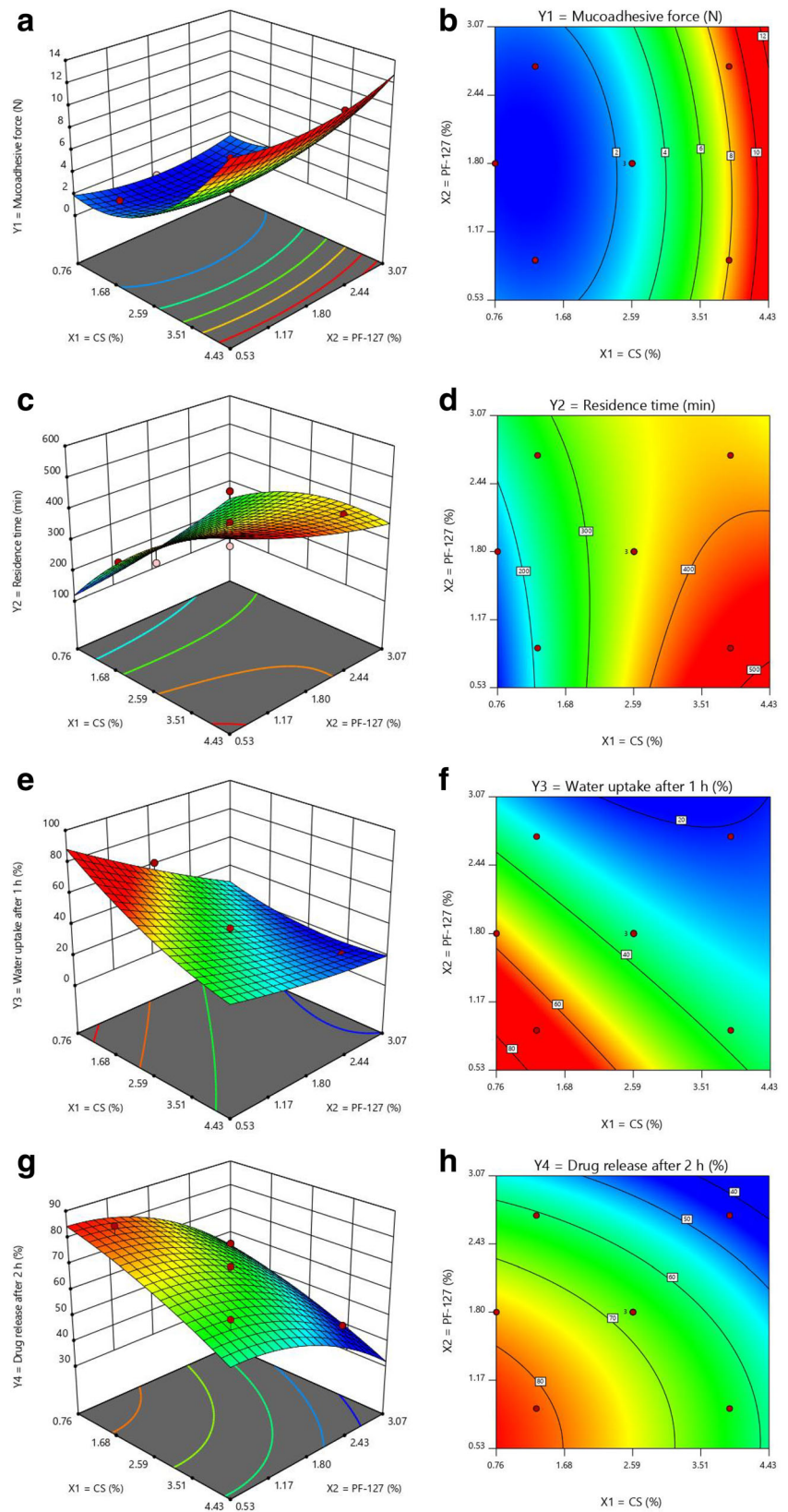
Model	$Y_1$		$Y_2$		$Y_3$		$Y_4$	
	<i>R</i> -squared	Adjusted <i>R</i> -squared	<i>R</i> -squared	Adjusted <i>R</i> -squared	<i>R</i> -squared	Adjusted <i>R</i> -squared	<i>R</i> -squared	Adjusted <i>R</i> -squared
Linear	0.8396	0.7996	0.7640	0.7050	0.9056	0.8821	0.9002	0.8753
2FI	0.8408	0.7726	0.8228	0.7468	0.9471	0.9244	0.9005	0.8578
Quadratic <sup>a</sup>	0.9632	0.9263	0.8939	0.7877	0.9688	0.9375	0.9476	0.8953
Quadratic model	Estimate	<i>P</i> value	Estimate	<i>P</i> value	Estimate	<i>P</i> value	Estimate	<i>P</i> value
Intercept	$\beta$		$\beta$		$\beta$		$\beta$	
$X_1$	2.54	–	350.78	–	35.51	–	67.23	–
$X_2$	+ 3.66	0.0001*	+ 91.6903	0.0019*	– 10.5707	0.0007*	– 8.6177	0.0018*
$X_1X_2$	+ 0.1998	0.5859	– 7.5073	0.6452	– 13.5382	0.0002*	– 9.9570	0.0009*
$X_1^2$	+ 0.1925	0.7081	– 36.0850	0.1570	+ 5.1950	0.0497*	+ 0.2850	0.8927
$X_2^2$	+ 1.6637	0.0096*	– 28.6158	0.1777	+ 3.1642	0.1214	– 1.3083	0.4739
	+ 0.5562	0.2316	+ 8.0492	0.6776	+ 1.0142	0.5763	– 3.5783	0.0879

$X_1$  = CS,  $X_2$  = PF-127;  $Y_1$  = Ex vivo mucoadhesive force;  $Y_2$  = Ex vivo residence time;  $Y_3$  = In vitro water uptake after 1 h;  $Y_4$  = In vitro drug release after 2 h

<sup>a</sup> Selected model

\* Significant effect of factors on individual responses

**Fig. 1** 3D response surface plots and their corresponding contour plots showing the effects of the factors on responses: **a, b** ex vivo mucoadhesion force; **c, d** ex vivo residence time; **e, f** in vitro water uptake after 1 h; and **g, h** in vitro drug release after 2 h



**Ex Vivo Residence Time** The ex vivo residence time is an essential parameter used to estimate the permanence of a mucoadhesive drug delivery system at its application site

and to ensure effective drug treatment. The ex vivo residence time ( $Y_2$ ) of the MT-MBPs varied between  $114.67 \pm 20.03$  and  $442.67 \pm 36.67$  min, as shown in Table 3.

Equation 7 describes the relationship between factors and responses, as follows:

$$Y_2 = 350.78 + 91.69X_1 - 7.50X_2 - 36.08X_1X_2 - 28.61X_1^2 + 8.04X_2^2 \quad (7)$$

The results indicated that  $X_1$  had a positive significant influence on  $Y_2$  (Table 4). Rapid gel formation was observed in patches containing low concentrations of CS and these were rapidly detached from the porcine buccal tissue [30]. Moreover, the union between MT-MBPs and mucosa was unstable due to the small number of CS molecules that penetrated per unit volume of the mucosa, resulting in short residence times. When the CS concentration was higher, the active sites available for the union between MT-MBPs and mucosa increased, leading to longer residence times. 3D response surface and contour plots for the ex vivo residence time are displayed in Fig. 1c and d.

**In Vitro Water Uptake After 1 h** The in vitro water uptake test allows for investigators to know the capacity of patches to absorb the surrounding medium as well as the subsequent formation of a gel barrier, which limits drug release. The water uptake profiles of the MT-MBPs are given in Fig. 2a. It was seen that the CS-based polymer matrix rapidly absorbed the SSF medium, increasing its weight as a function of time, and the physical integrity of the MT-MBPs remained intact during the whole water uptake study. After 4 h of exposure to the SSF medium, the water uptake of the MT-MBPs ranged from  $23.90 \pm 5.75$  to  $69.73 \pm 8.29\%$ . It was also observed that the patches with the highest concentrations of both PF-127 and CS exhibited the lowest water uptake percentages.

The maximum water uptake percentage reached by every formulation was found to be close to 1 h. By considering all formulations presented in Table 3, the water uptake percentage after 1 h ( $Y_3$ ) remained between  $19.31 \pm 5.55$  and  $64.27 \pm 10.26$ . The mathematical model describing the relationship between factors and this response is given in Eq. 8, as follows:

$$Y_3 = 35.51 - 10.57X_1 - 13.53X_2 + 5.19X_1X_2 + 3.16X_1^2 + 1.01X_2^2 \quad (8)$$

The factors  $X_1$  and  $X_2$  as well as the interaction  $X_1X_2$  had significant effects on  $Y_3$  (Table 4). The negative coefficients of  $X_1$  and  $X_2$  indicated that an increase in either factor led the water uptake to decrease. Poloxamers at low concentrations ( $10^{-4} - 10^{-5}\%$ ) form monomolecular micelles, while, at higher concentrations, the micelles become ordered, giving rise to multimolecular aggregates and forming a lattice [31]. Therefore, the inverse effect of  $X_2$  on  $Y_3$  could be attributed to the lattice formed by PF-127 in the CS-based polymer matrix. On the other hand, the inverse effect on the water uptake provoked by a high CS concentration in the MT-MBPs could be due to the low water solubility of CS. 3D response surface and contour plots presenting the effect of the PF-127 concentration and CS concentration on the in vitro water uptake percentage after 1 h are illustrated in Fig. 1e and f.

**In Vitro Drug Release After 2 h** The drug release profiles of the MT-MBPs are given in Fig. 2b. It can be seen that there was an initial burst release between  $19.78 \pm 2.15$  and  $41.86 \pm 2.22\%$  after 30 min, followed by a sustained release for up to 8 h. The initial burst release might be ascribed to the rapid release of drug molecules attached to the surface of the mucoadhesive layer. After 8 h, the cumulative drug release ranged from  $92.05 \pm 4.20$  to  $96.73 \pm 2.36\%$ .

The drug release data were fitted to zero order, first order, Higuchi, and Korsmeyer–Peppas models, as depicted in Table 5. From these results, the best-fit model to explain the MT release behavior was the Higuchi model, which is frequently employed for describing the drug release from matrix-type systems such as ointments films, thin films, and transdermal patches [32]. The diffusion exponent ( $n$ ) values from the Korsmeyer–Peppas model were found to be in the range of 0.406 to 0.537. According to these results, it might be established that drug release from the CS-based polymer matrix was controlled by Fickian diffusion through micropores filled with the release medium, which are present within the polymer matrix [33, 34].

**Fig. 2** a In vitro water uptake profiles of the MT-MBPs and b in vitro drug release profiles of the MT-MBPs

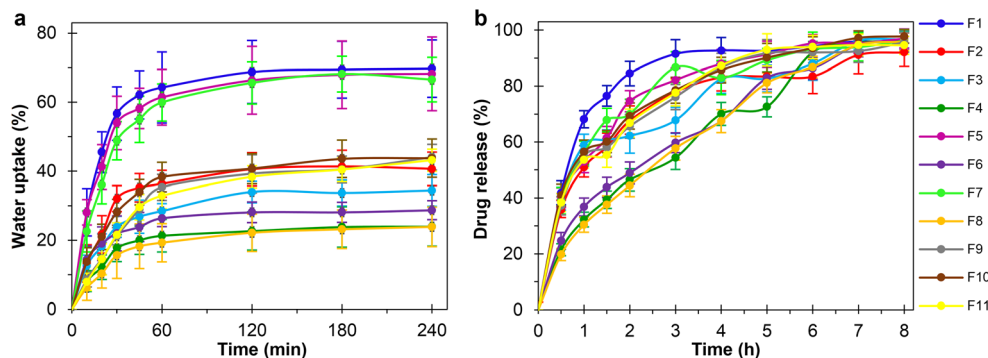




**Table 5** Model fitting for the kinetics of drug release of the MT-MBPs prepared as per CCD

Code	Zero order	First order			Higuchi		Korsmeyer–Peppas		
	$M_t = M_0 + K_0 t$	$Ln M_t = Ln M_0 + K_1 t$			$M_t/M_\infty = K_H \times t^{1/2}$		$M_t/M_\infty = K_{KP} \times t^n$		
	R-squared	$K_0$	R-squared	$K_1$	R-squared	$K_H$	R-squared	$K_{KP}$	n value
F1	0.597	2.53	0.511	0.071	0.987	0.675	0.972	7.846	0.507
F2	0.816	3.22	0.725	0.098	0.998	0.444	0.989	7.768	0.453
F3	0.921	3.39	0.841	0.097	0.965	0.515	0.918	10.278	0.406
F4	0.965	5.11	0.885	0.182	0.994	0.324	0.985	3.525	0.537
F5	0.816	3.44	0.735	0.098	0.991	0.456	0.988	9.776	0.486
F6	0.964	4.74	0.878	0.162	0.995	0.326	0.984	4.953	0.491
F7	0.787	3.19	0.694	0.092	0.992	0.556	0.983	9.116	0.481
F8	0.965	5.19	0.869	0.191	0.997	0.366	0.987	2.746	0.518
F9	0.851	3.53	0.767	0.103	0.956	0.465	0.947	10.381	0.482
F10	0.882	3.49	0.802	0.098	0.952	0.453	0.953	12.183	0.493
F11	0.845	3.62	0.781	0.105	0.976	0.447	0.945	11.023	0.483

$M_0$  is the initial drug amount in the patches;  $M_t$  is amount of drug released at time  $t$ ;  $M_\infty$  is the amount of drug released at infinite time;  $K_0$  is the zero-order release constant;  $K_1$  is the first order release constant;  $K_H$  is the Higuchi release constant;  $K_{KP}$  is the Korsmeyer–Peppas release constant; and  $n$  is the diffusion exponent indicative of drug release mechanism

The in vitro drug release after 2 h ( $Y_4$ ) ranged between  $44.43 \pm 3.96$  and  $84.48 \pm 4.35\%$ , as depicted in Table 3. The effects of factors on  $Y_4$  can be explained by the following (Eq. 9):

$$Y_4 = 67.23 - 8.61X_1 - 9.95X_2 + 0.28X_1X_2 - 1.30X_1^2 - 3.57X_2^2 \quad (9)$$

The concentrations of CS and PF-127 had an inverse significant effect on drug release (Table 4) that is, when either  $X_1$  or  $X_2$  increased, a significant decrease in  $Y_4$  was observed. When the CS concentration in the MT-MBPs was high, a stronger gel barrier was produced, making drug diffusion more difficult [30]. In addition, a multimolecular lattice within the CS-based polymer matrix could be formed at high PF-127 concentrations, producing a more viscous system, which decreased the in vitro drug release. 3D response surface and contour plots related to in vitro drug release are presented in Fig. 1g and h.

**Thickness, Surface pH, Folding Endurance, Moisture Content, and Drug Content** The obtained results from thickness, surface pH, folding endurance, moisture content, and drug content of the MT-MBPs prepared as per the experimental design matrix are shown in Table 3. Thickness was in the range of  $587 \pm 35.92$  to  $789 \pm 47.95 \mu\text{m}$ , which suggests thickness uniformity. All patches prepared had a surface pH value close to 6.8, so they were expected to be non-irritating to the buccal mucosa. The folding endurance was greater than 200, which is a sign of adequate

flexibility. The moisture content remained between  $2.10 \pm 0.34$  and  $3.80 \pm 0.75\%$ , indicating very good integrity during storage. Additionally, the drug content ranged from  $95.27 \pm 1.77$  to  $97.74 \pm 1.75\%$ , which demonstrates the performance of the solvent casting method in preparing the MT-MBPs with high drug entrapment efficiencies.

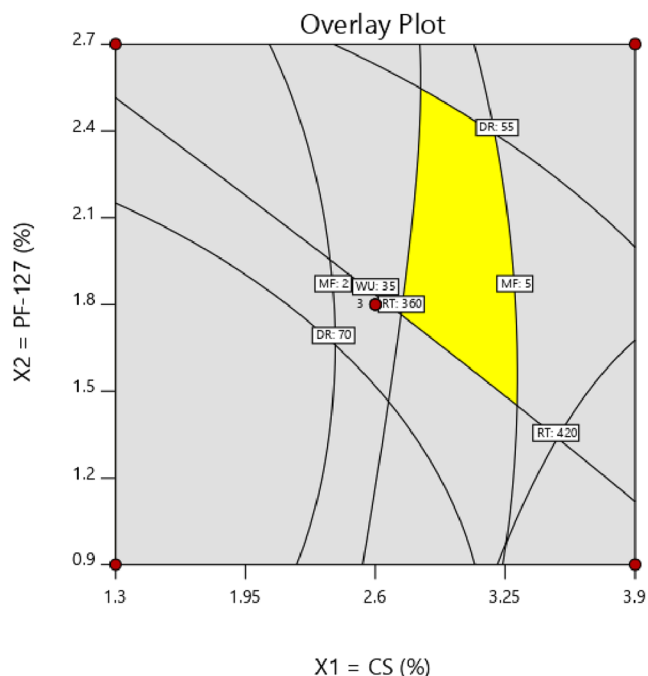


**Fig. 3** Overlay plot between the two factors across two-dimensional (2D) experimental domain for responses

**Table 6** Comparison between predicted and observed responses of the optimized MT-MBPs

Response	Predicted value	Observed value	95% prediction interval	Predicted error (%) <sup>a</sup>
Y <sub>1</sub>	3.97	3.58	2.63–5.31	9.82
Y <sub>2</sub>	360.66	342.67	300.85–420.47	4.98
Y <sub>3</sub>	22.91	24.53	17.34–28.47	7.07
Y <sub>4</sub>	53.38	51.89	47.84–58.92	2.79

Y<sub>1</sub> = Ex vivo mucoadhesive force; Y<sub>2</sub> = Ex vivo residence time; Y<sub>3</sub> = In vitro water uptake after 1 h; Y<sub>4</sub> = In vitro drug release after 2 h

CS = 2.9% (w/v); PF-127 = 2.6% (w/v)

<sup>a</sup> Predicted error (%) = [(Predicted value – Observed value)/Predicted value] × 100

**Formulation Optimization** The Design Expert® software was used to optimize the formulation variables by applying the corresponding constraints to responses and solving the polynomial equations. Overlay plot was produced, where the yellow segment offers a formulation with demanded attributes as per the constraints (Fig. 3). From mathematical and graphical analyses, the optimal levels of independent variables were found to be 2.9% (w/v) and 2.6% (w/v) for CS and PF-127, respectively, predicting an ex vivo mucoadhesive force of 3.97 N, an ex vivo residence time of 360.66 min, an in vitro water uptake after 1 h of 22.91%, and an in vitro drug release after 2 h of 53.38%, with an overall desirability of 1.000. Taking into consideration these findings, the optimized MT-MBPs were prepared and their observed responses are displayed in Table 6. It was found that the observed responses were in agreement with the predicted values and within the 95% prediction interval, confirming the predictability and validity of the model.

### Characterization and Evaluation of the Optimized Formulation

Characterization of the optimized MT-MBPs is presented in Table 7. These results demonstrated that optimized MT-MBPs presented desired properties in terms of mucoadhesive force, residence time, water uptake, drug release, thickness, pH surface, folding endurance, moisture content, and drug content. Figure 4a contains the in vitro water uptake profile and in vitro drug release profile from the optimized MT-MBPs. On the one hand, the in vitro water uptake after 1 h was close to 25%, allowing for control of the ex vivo residence time and in vitro

drug release. On the other hand, the percentage of drug released from the optimized MT-MBPs was 51% during the first 2 h, reaching 91% of drug release until the end of the test (8 h). In addition, these data were well fitted to both the Higuchi ( $R$ -squared = 0.9975) and the Korsmeyer–Peppas ( $R$ -squared = 0.9821,  $n = 413$ ) models, implying a drug release mechanism controlled by a diffusion process. Considering the performance of the optimized MT-MBPs, it can be concluded that they are highly recommended to be used as an innovative buccal drug delivery system.

**SEM Analysis** SEM images showed that the optimized MT-MBPs had a microporous surface with no structural cracks and drug-free crystals (Fig. 5a–d), confirming the homogeneous distribution of MT into the CS-based polymer matrix.

**DSC Analysis** The DSC thermograms are given in Fig. 5e. MT had an endothermic peak at 122 °C correlated with the melting point [35]. The thermogram of CS exhibited two endothermic peaks at 70 °C and 175 °C, indicating a loss of unbound and bound water, respectively [36]. PF-127 presented a melting peak at 58 °C that confirmed the crystalline nature of the polymer [37]. On the other hand, the complete disappearance of MT characteristic peak in the thermogram of the optimized MT-MBPs corroborated the molecular dispersion of the MT into the CS-based polymer matrix possibly in an amorphous or disordered crystalline form.

**Mechanicals Properties** The mechanical properties of buccal patches are fundamental attributes, since they may foretell

**Table 7** Characterization of the optimized MT-MBPs

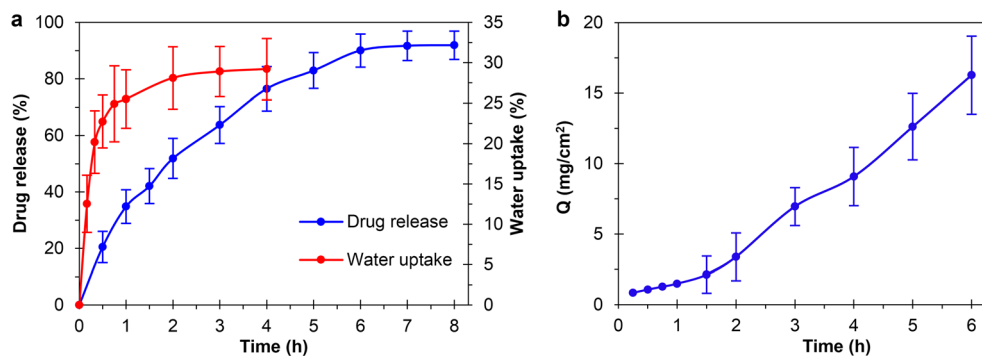
Mucoadhesive force <sup>a</sup> (N)	Residence time <sup>b</sup> (min)	Water uptake after 1 h <sup>b</sup> (%)	Drug release after 2 h <sup>b</sup> (%)	Thickness <sup>c</sup> (μm)	Surface pH <sup>b</sup> –	Folding endurance <sup>b</sup> (No.)	Moisture content <sup>b</sup> (%)	Drug content <sup>b</sup> (%)
3.58 ± 0.62	342.67 ± 17.21	24.53 ± 3.62	51.89 ± 7.12	748.3 ± 25.83	6.24 ± 0.11	265 ± 11	3.14 ± 0.66	96.24 ± 1.13

<sup>a</sup> Values are presented as mean ± SD,  $n = 6$

<sup>b</sup> Mean ± SD,  $n = 3$

<sup>c</sup> Mean ± SD,  $n = 10$

**Fig. 4** **a** In vitro water uptake profile and in vitro drug release profile of the optimized MT-MBPs. **b** Ex vivo drug permeation profile of the optimized MT-MBPs



stability, drug release, and adhesion to the buccal mucosa. An exemplary buccal patch should be flexible, elastic, and sufficiently strong so as to resist rupture due to the tension generated during its permanence in the buccal cavity [38]. In this sense, the tensile strength and elongation at break can describe the strength and elasticity of a film [39]. The tensile strength and elongation at break values of the optimized MT-MBPs were  $3.76 \pm 0.55$  N/mm<sup>2</sup> and  $36.52 \pm 13.88\%$ , respectively. These values showed that the mechanical properties of the MT-MBPs were suitable to withstand the stress that prevails in the buccal cavity.

**Ex Vivo Drug Permeation** The ex vivo drug permeation studies were carried out to establish the systemic absorption of the drug through the buccal epithelium. Results of the ex vivo drug permeation from the optimized MT-MBPs revealed that the maximum permeation flux ( $J_{SS}$ ) was  $3,100 \pm 214.5$   $\mu\text{g}/\text{cm}^2/\text{h}$  with a lag time ( $t_L$ ) of  $0.87 \pm 0.09$  h and a permeability coefficient ( $K_p$ ) of  $0.0644 \pm 4.45 \times 10^{-3}$  cm/h. Figure 4b contains the drug permeation profile. The optimized MT-MBPs provided a prolong residence time that promotes drug permeability. The probable mechanism of action of CS in improving transmucosal drug transport could be related to the capacity of CS to alter the lipid arrangement in the buccal epithelium. The

positive charges of CS interact with cell membranes, which leading to a structural rearrangement of tight junction-associated proteins [40, 41]. On the other hand, poloxamers have been shown to function as a permeation-enhancing agent. These polymers may insert into lipid membranes, changing the lateral packing density of membranes and enhancing drug absorption [42]. Based on the ex vivo permeation results, therapeutic concentrations of MT can be reached by using the optimized MT-MBP are of  $5.62$  cm<sup>2</sup>.

## Conclusion

In this study, MT-MBPs were prepared using the solvent casting method and successfully optimized via a certain experimental approach. The CCD provided a high level of prediction, suggesting that the CS and PF-127 mixtures can successfully regulate the properties of the MT-MBPs. The optimized formulation factors obtained from this study were 2.9% (w/v) of CS and 2.6% (w/v) of PF-127. The SEM and DSC evaluations showed that MT was homogeneously dispersed into the microporous CS-based polymer matrix. The thickness of the MT-MBPs could turn out to be quite comfortable for the patient. The mucoadhesive and water uptake properties were

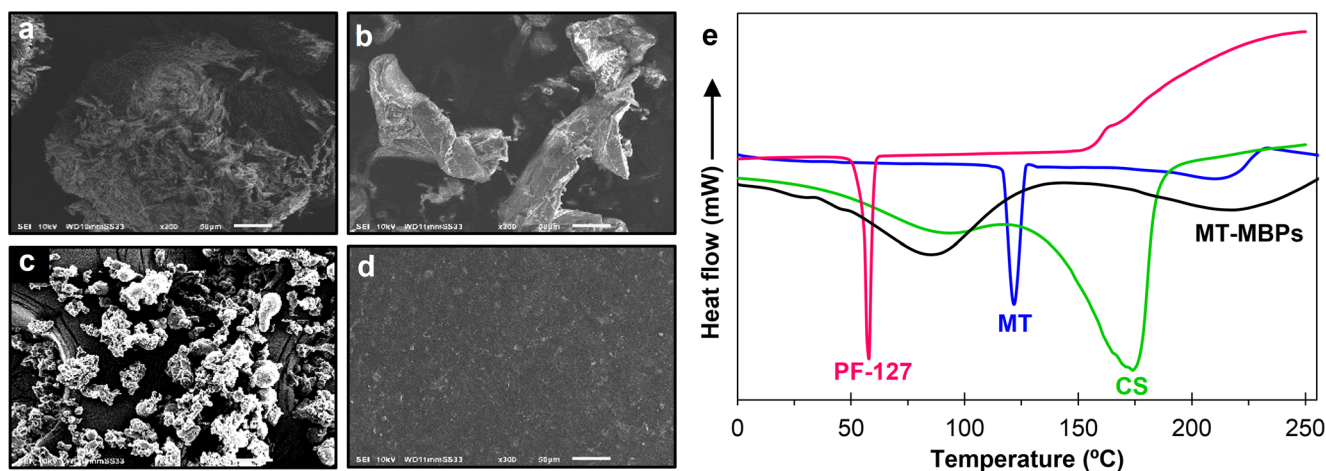


**Fig. 5** SEM micrographs of **a** MT, **b** CS, **c** PF-127, and **d** optimized MT-MBPs. **e** DSC thermograms of the drug, excipients, and the optimized MT-MBPs. The scale bar represents 50  $\mu\text{m}$

found be satisfactory. The optimized MT-MBPs exhibited a controlled drug release for 8 h. The mechanical properties were suitable to withstand the stress in the buccal cavity and to help avoid the feeling of discomfort after application. The appropriate area of the MT-MBPs should be 5.62 cm<sup>2</sup> for the successful control of the drug dosage. However, future in vivo studies need to be performed in order to correlate our results. Finally, the optimized MT-MBPs developed in the present work can be considered as a potential alternative for MT delivery in the treatment of different cardiovascular diseases.

**Acknowledgments** Dr. Escobar Chávez wants to acknowledge PAPIIT IT/UNAM [200218]; Cátedra PIAP I [1817]; and PIAPIME [2.12.27.19].

**Availability of Data and Materials** All data generated or analyzed in this study are included in this manuscript.

### Compliance with Ethical Standards

**Conflict of Interest** The authors declare that they have no conflict of interest.

**Abbreviations** MT, metoprolol tartrate

MBPs

mucoadhesive buccal patches

MT-MBPs

mucoadhesive buccal patches loaded with metoprolol

CS

chitosan

PF-127

Pluronic® F-127

EC

ethyl cellulose

Eu-E100

Eudragit® E-100

RSM

response surface methodology

CCD

central composite design

SEM

scanning electron microscopy

DSC

differential scanning calorimetry

SSF

simulated salivary fluid

ANOVA

analysis of variance

### References

- Patel VF, Liu F, Brown MB. Advances in oral transmucosal drug delivery. *J Control Release*. 2011;153:106–16.
- Hearnden V, Sankar V, Hull K, Juras DV, Greenberg M, Kerr AR, et al. New developments and opportunities in oral mucosal drug delivery for local and systemic disease. *Adv Drug Deliv Rev*. 2012;64:16–28.
- Smart JD. Buccal drug delivery. *Expert Opin Drug Deliv*. 2005;2:507–17.
- Ikeuchi-Takahashi Y, Ishihara C, Onishi H. Evaluation of polyvinyl alcohols as mucoadhesive polymers for mucoadhesive buccal tablets prepared by direct compression. *Drug Dev Ind Pharm*. 2017;43:1489–500.
- Cevher E, Taha MA, Orlu M, et al. Evaluation of mechanical and mucoadhesive properties of clomiphene citrate gels formulations containing carbomers and their thiolated derivatives. *Drug Deliv*. 2008;15:57–67.
- Kumria R, Al-Dhubiab BE, Shah J, et al. Formulation and evaluation of chitosan-based buccal bioadhesive films of zolmitriptan. *J Pharm Innov*. 2018;13:133–43.
- Morales JO, McConville JT. Manufacture and characterization of mucoadhesive buccal films. *Eur J Pharm Biopharm*. 2011;77:187–99.
- Kumria R, Nair AB, Goomber G, Gupta S. Buccal films of prednisolone with enhanced bioavailability. *Drug Deliv*. 2016;23:471–8.
- Mati-Baouche N, Pierre-Henri E, Baynast H, et al. Chitosan as an adhesive. *Eur Polym J*. 2014;60:198–212.
- Pitto-Barry A, Barry NPE. Pluronic® block-copolymers in medicine: from chemical and biological versatility to rationalization and clinical advances. *Polym Chem*. 2014;10:2381–496.
- Dumortier G, Grossiord JL, Agnely F, Chaumeil JC. A review of poloxamer 407 pharmaceutical and pharmacological characteristics. *Pharm Res*. 2006;23:2709–28.
- Abou el ela ael S, Allam AA, Ibrahim EH. Pharmacokinetics and anti-hypertensive effect of metoprolol tartrate rectal delivery system. *Drug Deliv*. 2016;23:69–78.
- Ripley TL, Saseen JJ.  $\beta$ -Blockers: a review of their pharmacological and physiological diversity in hypertension. *Ann Pharmacother*. 2014;48:723–33.
- Grassi G. Metoprolol in the treatment of cardiovascular disease: a critical reappraisal. *Curr Med Res Opin*. 2018;34:1635–43.
- Fernandes GJ, Rathnanand M. *J Pharm Innov*. Formulation optimization for gastroretentive drug
- Abul Kalam M, Khan AA, Khan S, Almalik A, Alshamsan A. Optimizing indomethacin-loaded chitosan nanoparticle size, encapsulation, and release using Box–Behnken experimental design. *Int J Biol Macromol*. 2016;87:329–40.
- Parhi R, Panamukhy T. RSM-based design and optimization of transdermal film of ondasteron HCl. *J Pharm Innov*. 2019. <https://doi.org/10.1007/s12247-019-09373-9>.
- Box GPE, Wilson KB. On the experimental attainment of optimum conditions. *J Roy Stat Soc Ser B*. 1951;13:1–45.
- Escobar-Chávez JJ, Merino V, Diez-Sales O, et al. Transdermal nortriptyline hydrochloride patch formulated within a chitosan matrix intended to be used for smoking cessation. *Pharm Dev Technol*. 2011;16:162–9.
- Patel VF, Liu F, Brown MB. Modeling the oral cavity: in vitro and in vivo evaluations of buccal drug delivery systems. *J Control Release*. 2012;161:746–56.
- Perioli L, Ambrogio V, Angelici F, Ricci M, Giovagnoli S, Capuccella M, et al. Development of mucoadhesive patches for buccal administration of ibuprofen. *J Control Release*. 2004;99:73–82.
- El-Fek GS, Farouk Abdulmaguid R, Zayed GM, et al. Mucosal co-delivery of ketorolac and lidocaine using polymeric wafers for dental application. *Drug Deliv*. 2018;25:35–42.
- Shiledar RR, Tagalpallewar AA, Kokare CR. Formulation and in vitro evaluation of xanthan gum-based bilayered mucoadhesive



- buccal patches of zolmitriptan. *Carbohydr Polym.* 2014;101:1234–42.
24. Nair AB, Kumria R, Harsha S, Attimarad M, al-Dhubiab BE, Alhaider IA. In vitro techniques to evaluate buccal films. *J Control Release.* 2013;166:10–21.
  25. Adhikari SN, Nayak BS, Nayak AK, et al. Formulation and evaluation of buccal patches for delivery of atenolol. *AAPS PharmSciTech.* 2010;11:1038–44.
  26. Yildiz Pekoz A, Sedef Erdal M, Okyar A, Ocak M, Tekeli F, Kaptan E, et al. Preparation and in-vivo evaluation of dimenhydrinate buccal mucoadhesive films with enhanced bioavailability. *Drug Dev Ind Pharm.* 2016;42:916–25.
  27. Samson G, de la García Calera A, Dupuis-Girod S, et al. Ex vivo study of bevacizumab transport through porcine nasal mucosa. *Eur J Pharm Biopharm.* 2012;80:465–9.
  28. Huang Y, Leobandung W, Fross A, et al. Molecular aspects of muco- and bioadhesion: tethered structures and site-specific surfaces. *J Control Release.* 2000;65:63–71.
  29. Khutoryanskiy VV. Advances in mucoadhesion and mucoadhesive polymers. *Macromol Biosci.* 2011;11:748–64.
  30. Shidhaye SS, Saindane NS, Sutar S, Kadam V. Mucoadhesive bilayered patches for administration of sumatriptan succinate. *AAPS PharmSciTech.* 2008;9:909–16.
  31. Escobar-Chávez JJ, López-Cervantes M, Naik A, et al. Applications of thermo-reversible pluronic F-127 gels in pharmaceutical formulations. *J Pharm Pharm Sci.* 2006;9:339–58.
  32. Siepmann J, Peppas NA. Higuchi equation: derivation, applications, use and misuse. *Int J Pharm.* 2011;418:6–12.
  33. Gurny R, Doelker E, Peppas NA. Modelling of sustained release of water-soluble drugs from porous, hydrophobic polymers. *Biomaterials.* 1982;3:27–32.
  34. Korsmeyer RW, Gurny R, Doelker E, Buri P, Peppas NA. Mechanisms of solute release from porous hydrophilic polymers. *Int J Pharm.* 1983;15:25–35.
  35. Varshosaz J, Faghihian H, Rastgoo K. Preparation and characterization of metoprolol controlled-release solid dispersions. *Drug Deliv.* 2006;13:295–302.
  36. Helmy AM, Elsbahy M, Soliman GM, et al. Development and in vivo evaluation of chitosan beads for the colonic delivery of azathioprine for treatment of inflammatory bowel disease. *Eur J Pharm Sci.* 2017;109:269–79.
  37. Mendosa NS, Murthy SN, Hashemnejad SM, et al. Development of poloxamer gel formulations via hot-melt extrusion technology. *Int J Pharm.* 2018;537:122–31.
  38. Palem CR, Gannu R, Doodipala N, Yamsani VV, Yamsani MR. Transmucosal delivery of domperidone from bilayered buccal patches: in vitro, ex vivo and in vivo characterization. *Arch Pharm Res.* 2011;34:1701–10.
  39. Lim H, Hoag SW. Plasticizer effects on physical-mechanical properties of solvent cast Soluplus® films. *AAPS PharmSciTech.* 2013;14:903–10.
  40. Senel S, Kremer MJ, Kaş S, et al. Enhancing effect of chitosan on peptide drug delivery across buccal mucosa. *Biomaterials.* 2000;21:2067–71.
  41. Bernkop-Schnürch A, Dünnhaupt S. Chitosan-based drug delivery systems. *Eur J Pharm Biopharm.* 2012;81:463–79.
  42. Seelig A, Gerebtzoff G. Enhancement of drug absorption by noncharged detergents through membrane and P-glycoprotein binding. *Expert Opin Drug Metab Toxicol.* 2006;2:733–52.

**Publisher's Note** Springer Nature remains neutral with regard to jurisdictional claims in published maps and institutional affiliations.